Contribution from the Inorganic Chemistry Laboratory,
University of Oxford, Oxford OX1 3QR, United Kingdom

Photochemical Reactions of $M(\eta\text{-}C_5H_5)_2L_n$ (M = W, Mo, Cr, V) in Low-Temperature Matrices. Detection of Tungstenocene and Molybdenocene

JENNIFER CHETWYND-TALBOT, PETER GREBENIK, and ROBIN N. PERUTZ*

Received January 29, 1982

Matrix-isolation methods with IR and UV/vis detection have been used to examine the primary photochemical products of MCp_2L_n (M = Mo, W, V; Cp = η-C_5H_5) compounds. In situ UV photolysis in Ar of WCp_2H_2, WCp_2D_2, $WCp_2(CH_3)H$, $WCp_2(C_2H_4)$, and WCp_2CO leads to a common product, WCp_2. UV photolysis of $MoCp_2H_2$, $MoCp_2D_2$, and $MoCp_2CO$ gives $MoCp_2$. The expelled ligands, CH_4, CO, and C_2H_4, all show evidence of perturbation by the metallocene in the same cage; no thermal recombination reactions are observed except with CO in Xe at ~60 K. Photolysis of MCp_2H_2 (M = Mo, W) in CO matrices gives MCp_2 and MCp_2CO. When M = W, no HCO is generated, indicating concerted expulsion of H_2; when M = Mo, a relatively small amount of HCO is observed. The spectra and reactions of MCp_2 (M = Mo, W) are compared to those for M = Cr, V. Chromocene and vanadocene react photochemically in CO matrices to form MCp_2CO; VCp_2CO reacts photochemically to give VCp_2 and CO in Ar matrices. The reactivity and the IR and the UV spectra of $MoCp_2$ and WCp_2 all indicate parallel sandwich structures. The IR spectra of $MoCp_2$ and $CrCp_2$ both exhibit broad bands and unusual intensity ratios, which are attributed to Jahn–Teller distortions of a $^3E_2$ ground state. The IR spectrum of WCp_2 is very similar to that of VCp_2 but has an additional broad, intense band at ~3240 cm^{-1}, which is shifted only 15 cm^{-1} on ^2H substitution. This band is assigned to a vibronically allowed electronic transition between spin–orbit substates of a $^3E_2$ ground state, in which the Jahn–Teller distortion is quenched by spin–orbit coupling. The UV spectra of MCp_2 (M = Mo, W) show two charge-transfer bands in the 300–420-nm region with a strong vibrational progression on the long-wavelength absorption. The metallocenes $MoCp_2$ and WCp_2 are postulated as the key intermediates in the C–H insertion reactions in solution.

Introduction

The technique of matrix isolation is a powerful method for the detection and identification of unstable reaction intermediates.[1] In this paper we report its application to identify the metallocene intermediates in the photochemistry of MCp_2L_n (M = Mo, W; Cp = η-C_5H_5) compounds. The use of IR and UV/vis spectroscopy allows us to deduce the molecular symmetry and electronic ground states of these metallocenes and to observe some simple thermal and photochemical reactions. These experiments give clues as to the causes of the striking increase in reactivity down the series MCp_2 (M = Cr, Mo, W), which culminates in the C–H insertion reactions of WCp_2. Some of this work has been reported in a preliminary communication.[2]

Solution photolysis of WCp_2H_2 or WCp_2CO in the presence of substrates such as benzene, mesitylene, or tetramethylsilane results in elimination of H_2 or CO and insertion of the WCp_2 unit into the aryl or alkyl C–H bonds.[3-5] Thermolysis of $WCp_2(CH_3)H$ results in elimination of CH_4 and generation of almost identical insertion products.[4] With substrates such as ethyne both substitution of H_2 by ethyne and insertion into arene solvents are observed, but in pure cyclohexane dimeric products are formed in which the tungsten atom has inserted into a C–H bond of a cyclopentadienyl ring. Similar reactions have been performed on the molybdenum system by photolysis of $MoCp_2H_2$ or $MoCp_2CO$ and by reduction of $MoCp_2Cl_2$ with sodium amalgam.[3,5] However, the dominant reaction is addition (e.g., with ethylene) and insertion is confined to the production of dimers similar to those of tungsten (see Chart I). The similarity of the reactions using a variety of MCp_2L_n precursors has led to the postulate of MCp_2 as the common intermediates in these reactions. Although these metallocenes have not been observed previously, they have been investigated theoretically by Brintzinger et al., who predicted a parallel structure and a ^3E ground state for $MoCp_2$.[6] The reactivity of the heavy metallocenes contrasts with that of chromocene, which maintains the $CrCp_2$ unit only in the labile addition complex with CO.[7]

Chart I

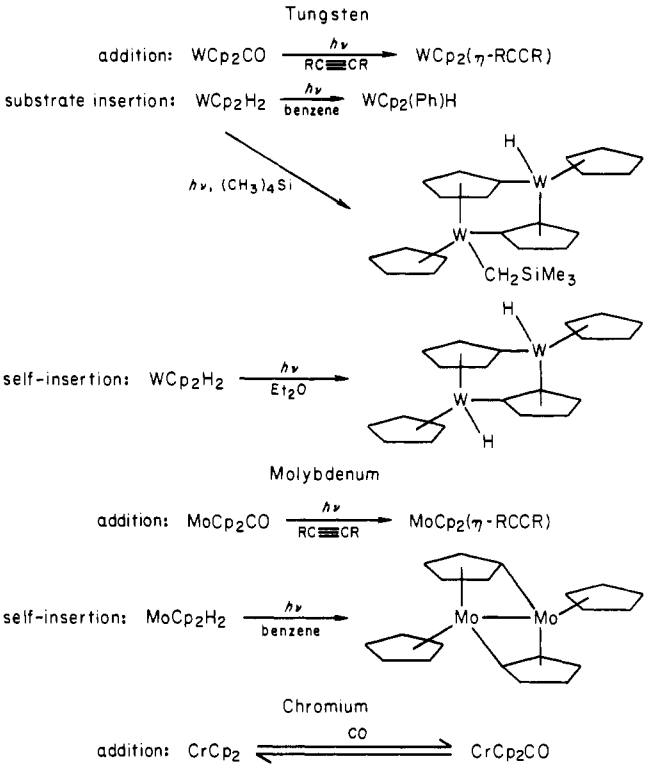

(1) Turner, J. J.; Burdett, J. K.; Perutz, R. N.; Poliakoff, M. *Pure Appl. Chem.* **1977**, *49*, 271. Downs, A. J.; Peake, S. C. *Mol. Spectrosc. (Chem. Soc., London)* **1973**, *1*, 523. Chadwick, B. M. *Ibid.* **1975**, *3*, 281; **1979**, *6*, 72.
(2) Grebenik, P.; Downs, A. J.; Green, M. L. H.; Perutz, R. N. *J. Chem. Soc., Chem. Commun.* **1979**, 742.
(3) Berry, M.; Cooper, N. J.; Green, M. L. H.; Simpson, S. J. *J. Chem. Soc., Dalton Trans.* **1980**, 29. Berry, M.; Elmitt, K.; Green, M. L. H. *Ibid.* **1979**, 1950.
(4) Cooper, N. J.; Green, M. L. H.; Mahtab, R. *J. Chem. Soc., Dalton Trans.* **1979**, 1557.
(5) Thomas, J. L.; Brintzinger, H. H. *J. Am. Chem. Soc.* **1972**, *94*, 1386. Wong, K. L. T.; Thomas, J. L.; Brintzinger, H. H. *Ibid.* **1974**, *96*, 3694. Thomas, J. L. *Ibid.* **1973**, *95*, 1838.
(6) Brintzinger, H. H.; Lohr, L. L.; Wong, K. L. T. *J. Am. Chem. Soc.* **1975**, *97*, 5146.

0020-1669/82/1321-3647$01.25/0

Further evidence concerning the photochemical reactions of MCp_2H_2 (M = Mo, W) has been obtained by Geoffroy and Bradley using 366-nm photolysis in benzene.[8] Their measurements give quantum yields of 0.1 ± 0.02 (Mo) and >0.01 ± 0.002 (W). Their isotopic studies indicate that expulsion of H_2 is the major process but some abstraction of ring and solvent protons also occurs, maybe in secondary reactions:

$$MoCp_2D_2 \xrightarrow[C_6H_6 \text{ or } C_6D_6]{h\nu} D_2/HD \ (1.6{:}1)$$

$$MoCp_2H_2 \xrightarrow[CD_3C_6D_5]{h\nu} H_2/HD \ (>9{:}1)$$

Experimental Section

Matrix-isolation experiments were carried out using an Air Products CS202 closed-cycle refrigerator cooling a CsI substrate. The system was pumped to $<3 \times 10^{-6}$ torr prior to cooling, and the operating pressure was better than 10^{-7} torr. The samples were sublimed from a heated glass side arm equipped with a high-vacuum tap (Apiezon T grease) and codeposited continuously with matrix gases (BOC research grade). The matrix gases were passed through a spiral trap (77 K) on the low-pressure side of the needle valve to remove condensables. However, water impurity bands were observed in most experiments. The matrices were deposited at a rate of 0.5–3.3 mmol h^{-1} for 2–4 h; deposition temperatures were 18–20 K for Ar, CO, N_2, and CH_4 but 25–30 K for Xe. IR spectra were measured on Perkin-Elmer 225 and 580 spectrophotometers, calibrated with atmospheric water vapor (frequencies ±1 cm^{-1}); UV/vis/near-IR spectra were recorded on a Perkin-Elmer 330 spectrophotometer. Samples were photolyzed through a silica window with a Philips HPK 125 W medium-pressure or a Hanovia high-pressure Hg arc. The radiation was filtered by H_2O (IR experiments) and on occasions a Calflex C filter ($\lambda > 375$ nm). The UV experiments were carried out with a front-silvered mirror but no water filter. There was no evidence for overheating of the matrix during photolysis.

The precursors MCp_2H_2 (M = Mo, W) were prepared by the method of Green and Knowles.[9] They were converted to MCp_2D_2 by reaction with dilute aqueous DCl, followed by precipitation with dilute NaOD. The resulting solid was recrystallized from toluene. The extent of deuteration was estimated by IR spectroscopy (Nujol mulls) to be ~90%, implying an isotope distribution $[M]D_2$:[M]HD ≈ 0.8:0.2.

Cyclopentadiene-d_6 was prepared with use of the procedure of Gallinella and Mirone.[10] Isotopic purity was estimated at better than 90% by gas-phase IR spectroscopy. After reaction with sodium sand in THF to give $Na^+C_5D_5^-$, it was used to synthesize $Mo(\eta\text{-}C_5D_5)_2H_2$ by the Green and Knowles route.[9] Analysis of the mass spectrum and IR spectrum (Nujol) indicated 90% deuteration of the rings. The resulting distribution of isotopomers should be D_{10}:D_9H:D_8H_2:D_7H_3 = 35:39:19:6. $W(\eta\text{-}C_5D_5)_2H_2$ was prepared by the reaction with D_2 in the presence of $Mn_2(CO)_{10}$ in toluene solution following Blickensderfer et al.[11] The product was extracted with HCl, precipitated with KOH, and recrystallized from toluene. The extent of deuteration was again estimated as 90 ± 2%. It should be noted that this approach failed to deuterate $MoCp_2H_2$.

$MoCp_2CO$ was prepared as described by Francis et al.[12] WCp_2CO was prepared by the same method, but the CO_2 was added at about 180 K rather than at room temperature.

$WCp_2(CH_3)H$ and $WCp_2(C_2H_4)$ were the generous gifts of Dr. M. Cannestrari and Mr. J. Bashkin, respectively.

VCp_2 and $CrCp_2$ were prepared by reaction of anhydrous metal trichlorides with $Na^+C_5H_5^-$ in THF as described by King.[13a] Vanadocene was converted to VCp_2CO by direct reaction with CO.[13b]

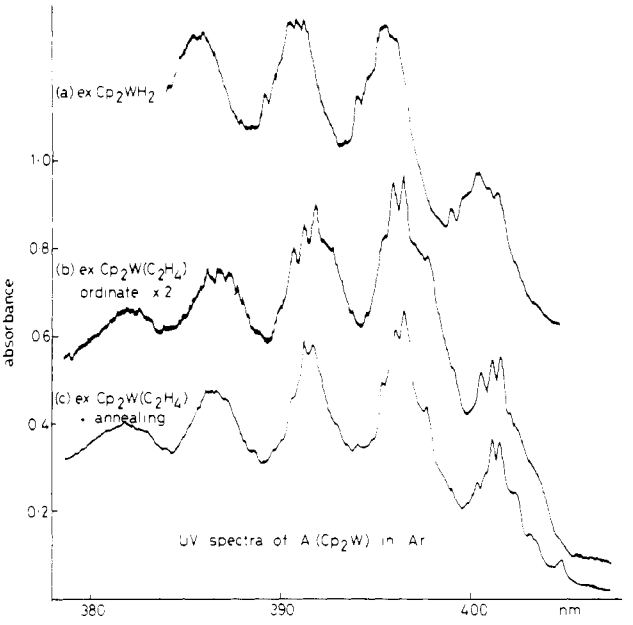

Figure 1. UV absorption spectra of the long-wavelength band of A (WCp_2) in Ar matrices at 20 K obtained as follows: (a) deposition of WCp_2H_2 followed by a 40-min UV photolysis with Philips HPK Hg arc; (b) deposition of $WCp_2(C_2H_4)$ followed by a 15-min UV photolysis (×2 ordinate expansion); (c) further 50-min photolysis of (b) followed by annealing to 36 K and recooling. There are no precursor absorptions in this region. Spectra b and c are recorded as difference spectra relative to the spectrum before photolysis, slit width 0.15–0.3 nm.

The sample sublimation temperatures are summarized in Table I.[14] For example, when $MoCp_2H_2$ was sublimed at 312 K and deposited with Ar for 4.5 h, the most intense band at 757 cm^{-1} had an absorbance of 1.49 and a full width at half-maximum (fwhm) of 3 cm^{-1}, but the low-frequency component of the Mo–H stretching mode at 1831 cm^{-1} had a fwhm of 18 cm^{-1}. A reduction of the sublimation temperature of 10 K and a 57% increase in the Ar deposited altered the absorbance at 757 cm^{-1} to 0.21 and the fwhm's to 4 and 15 cm^{-1}, respectively. Narrow bands below 1450 cm^{-1} and broad bands in the 1800–2000-cm^{-1} region are typical of both MCp_2H_2 and MCp_2CO (M = Mo, W). The M–H and C–O stretching modes appear to be far more sensitive to conformation or matrix trapping sites. However, the slight effect of a 10-fold dilution on the spectrum leads us to believe that we are dealing with monomeric species in all these experiments. The only exceptions are experiments on $MoCp_2H_2$ using simultaneous photolysis and deposition, in which extra product bands were observed (see below).

Results

In this paper we are concerned primarily with the photochemistry of MCp_2L_n (M = Mo, W) compounds. Details of the vibrational spectra of the precursor compounds will be presented elsewhere. Detailed assignments of the IR spectra of the products together with the spectra of all the stable metallocenes will also be published separately.

WCp_2H_2. When argon matrices doped with WCp_2H_2 were photolyzed for periods of 30–60 min with broad-band UV radiation, IR absorptions due to the starting material decreased in intensity to about 70% of their initial values and new bands assigned to a product A appeared (see Table II).[14] These new bands always appeared with the same intensity ratios. Taken with other observations described below, this indicates that they should be assigned to a single product. Neither photolysis with visible light nor annealing the matrix reversed the process. Complete conversion of starting material to A was not usually achieved even on prolonged photolysis, but complete conversion

(7) Wong, K. L. T.; Brintzinger, H. H. *J. Am. Chem. Soc.* **1975**, *97*, 5143.
(8) Geoffroy, G. L.; Bradley, M. G. *Inorg. Chem.* **1978**, *17*, 2410.
(9) Green, M. L. H.; Knowles, P. J. *J. Chem. Soc., Perkin Trans. 1* **1973**, 989.
(10) Gallinella, E.; Mirone, P. *J. Labelled Compd.* **1971**, *7*, 183.
(11) Blickensderfer, J. R.; Hoxmeier, R. J.; Kaesz, H. D. *Inorg. Chem.* **1979**, *18*, 3606.
(12) Francis, B. R.; Green, M. L. H.; Luong-Thi, T.; Moser, G. A. *J. Chem. Soc., Dalton Trans.* **1976**, 1339.
(13) (a) King, R. B. "Organometallic Syntheses"; Academic Press: New York, 1965; Vol. 1. (b) Calderazzo, F.; Fachinetti, G.; Floriani, C. *J. Am. Chem. Soc.* **1974**, *96*, 3695.

(14) See paragraph at end of the paper regarding supplementary material.

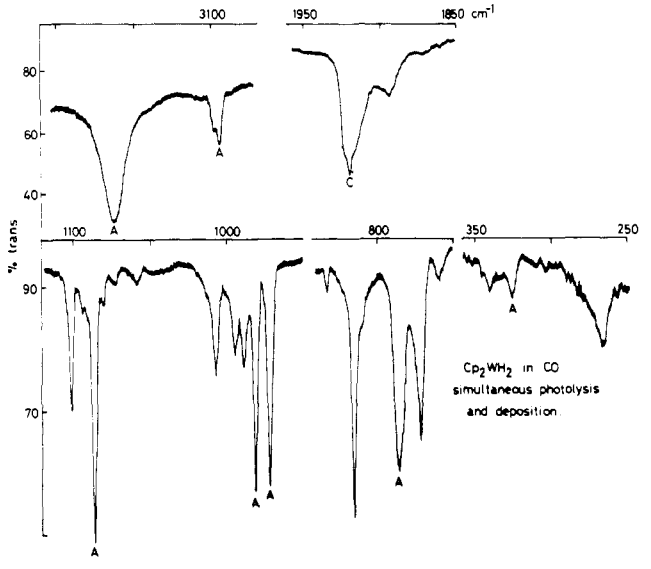

Figure 2. IR spectra recorded following 4-h codeposition of WCp_2H_2 and CO at 20 K with simultaneous Hg arc photolysis. Note ×2 ordinate expansion below 1150 cm^{-1}; A = WCp_2, and C = WCp_2CO, with unmarked bands due to WCp_2H_2.

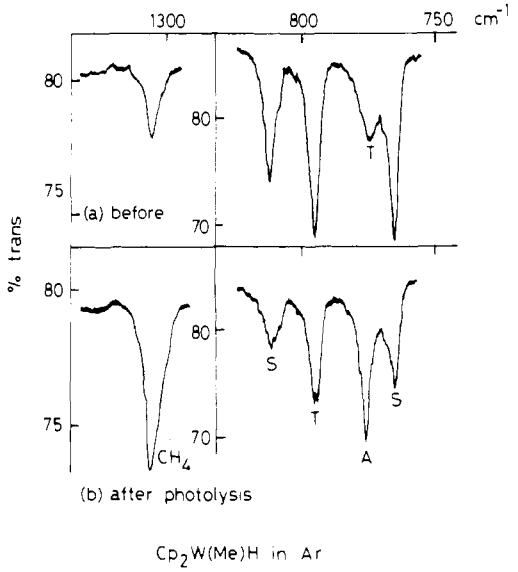

Figure 3. IR spectra recorded following (a) codeposition of $WCp_2(CH_3)H$ and Ar at 20 K and (b) 2.5-h Hg arc photolysis. Note ×2 ordinate expansion at left and ×5 ordinate expansion at right; A = WCp_2, S = WCp_2H_2 impurity, and T = $WCp_2(CH_3)H$.

was observed on one occasion when a lower sublimation temperature (45 °C) was combined with photolysis during deposition. In this case, the region 2000–1800 cm^{-1} associated with W–H stretching vibrations showed no absorptions. A similar experiment with WCp_2H_2 in Ar but with UV/vis/near-IR detection showed a decrease in the major absorption of the starting material at 268 nm and the growth of an intense structured product absorption peaking at 396 nm (see Tables III and IV).[14] An additional, more intense unstructured product band at ~328 nm overlapped the 330-nm shoulder of the starting material. The band at 396 nm showed five distinct members of a vibrational progression of mean frequency 321 cm^{-1} (Figure 1, Table IV). Superimposed on this structure were further splittings in the range 37–75 cm^{-1}, which were most conspicuous on the first member of the vibrational progression (Table V).[14] No other product bands were detected between 2600 and 405 nm. The two major bands at 396 and 323 nm, each with an extinction coefficient of $\sim 10^3$ (Table IV) are assigned to A. Their extinctions are estimated by comparing their intensities with the decrease in the bands of the starting material and assuming that the extinction coefficients of the precursor are the same as in hexane solution.[8]

The behavior observed for WCp_2H_2 in carbon monoxide matrices was different from that in argon. The most striking product band observed after photolysis for 1–2 h was a broad intense absorption at 1920 cm^{-1}. Absorptions due to the formation of A were also observed (see Table II). Deposition with photolysis produced similar results, but additional weak bands were detected at 874, 489, 484, 325, and 265 cm^{-1} (see Figure 2). On the basis of a comparison of the IR spectrum of an authentic sample of WCp_2CO in a carbon monoxide matrix, the bands at 1920, 874, 489, and 484 cm^{-1} may be assigned with certainty to this species while the bands at 325 and 265 cm^{-1} are assigned to A (Table VI).[14] No changes were observed in the IR spectrum on visible photolysis nor on annealing the matrix. Unlike comparable experiments with $ReCp_2H$ in CO, no band characteristic of HCO was observed at 1860 cm^{-1}.[15]

WCp_2D_2. On photolysis of WCp_2D_2 in argon, IR bands due to the product A were detected shifted by <1 cm^{-1} relative to those produced from WCp_2H_2.

$WCp_2(CH_3)H$. The sample of $WCp_2(CH_3)H$ was contaminated with WCp_2H_2. However, its presence did not interfere markedly with the experiments. Photolyzing with broad-band UV for 2.5 h led to a 50% decrease in intensity of bands due to $WCp_2(CH_3)H$ and a 60% decrease in bands of WCp_2H_2. Bands assigned to A appeared (see Table II), and a weak absorption initially present at 1305 cm^{-1} gained greatly in intensity (see Figure 3). This band may be assigned to the ν_4 mode of methane.[16] Evidently some $WCp_2(CH_3)H$ decomposed, releasing methane on sublimation (it decomposes in solution at 60–80 °C). The shift in band maximum from the literature value[16] of 1309.5 cm^{-1} to our observed 1305 cm^{-1} may indicate that the methane was interacting weakly with A. One photoproduct suggested by work on other transition-metal methyl complexes was the methyl radical.[17] Its most intense band has a broad contour in argon matrices, which makes it hard to detect, whereas it is sharp in solid dinitrogen (at 611 cm^{-1}).[18] UV photolysis of a matrix of $WCp_2(CH_3)H$ in a N_2 matrix led to the appearance of bands assigned to A (see Table II) and to both IR modes of methane (3018 (very weak, required ×10 ordinate expansion), 1306 cm^{-1}). No band was detected at 611 cm^{-1} when the maximum ordinate expansion available (×20) was used.

$WCp_2(C_2H_4)$. UV photolysis of Ar matrices containing $WCp_2(C_2H_4)$ led to the growth of new IR bands that may be assigned to A (see Table II) as well as absorptions at 3100, 2995, 1439, 1434, and 953 cm^{-1}, which may be assigned to ethene (literature values for C_2H_4 in solid argon, M:R 1:1000: 3111 (m), 3081 (w), 2995 (m), 1440 (s), 946 (vs), 807 (w) cm^{-1}).[19] The ethene in the matrix was obviously perturbed by A, and careful examination of the bands of A showed that it in turn was perturbed by the expelled ethene. This was particularly evident in the strongest absorption of A at 3240 cm^{-1} as well as in the 776-cm^{-1} band (see Figure 4). When the matrix was annealed to 38 K, all the bands showing evi-

(15) Milligan, D. E.; Jacox, M. E. *J. Chem. Phys.* **1964**, *41*, 3032; **1969**, *51*, 277.

(16) Cabana, A.; Savitsky, G. B.; Hornig, D. F. *J. Chem. Phys.* **1967**, *39*, 2942.

(17) Hudson, A.; Lappert, M. F.; Lednor, P. W.; Nicholson, B. K. *J. Chem. Soc., Chem. Commun.* **1974**, 966. Foust, D. F.; Rausch, M. D.; Samuel, E. *J. Organomet. Chem.* **1980**, *193*, 209.

(18) Milligan, D. E.; Jacox, M. E. *J. Chem. Phys.* **1967**, *47*, 5146.

(19) Barnes, A. J.; Howells, J. D. R. *J. Chem. Soc., Faraday Trans. 2* **1973**, *69*, 532.

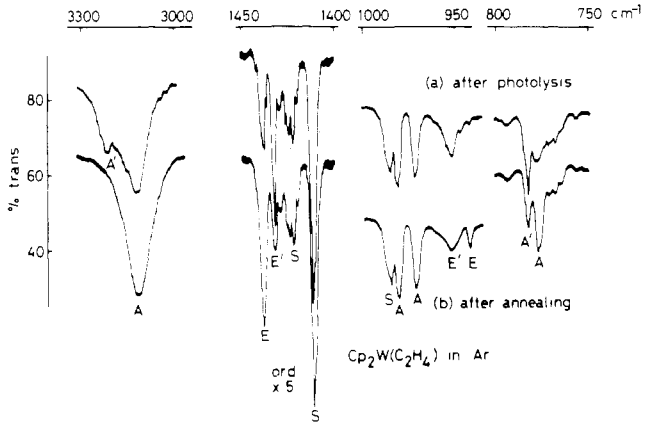

Figure 4. IR spectra recorded (a) following codeposition of $WCp_2(C_2H_4)$ and Ar at 20 K followed by a 30-min Hg arc photolysis and (b) after subsequent annealing to 30 K and recooling to 20 K. The ordinate of spectrum b is displaced by 20% with respect to (a). Note ×5 ordinate expansion between 1450 and 1400 cm^{-1}; S = $WCp_2(C_2H_4)$, A = WCp_2, A′ = perturbed WCp_2, E = C_2H_4, and E′ = perturbed C_2H_4.

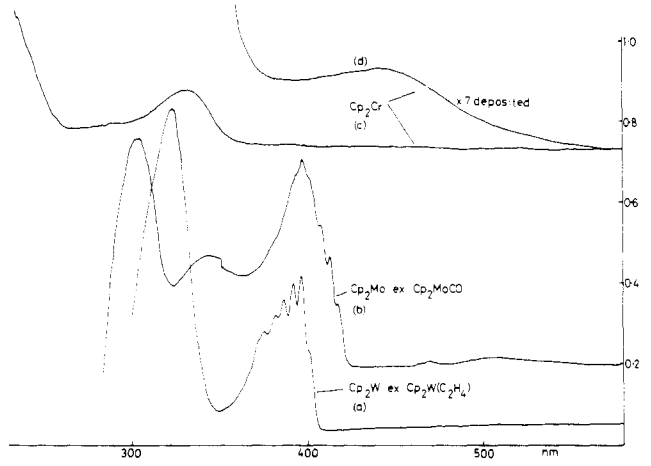

Figure 5. Low-resolution UV absorption spectra of (a) A (WCp_2) obtained following deposition of WCp_2H_2 in Ar followed by a 40-min photolysis, (b) M ($MoCp_2$) obtained following deposition of $MoCp_2CO$ in Ar followed by a 17-min photolysis, (c) $CrCp_2$ in Ar, and (d) $CrCp_2$ in Ar with 7 times as much material deposited as in (c), showing the d–d transition. Spectrum b is a difference spectrum relative to the spectrum before photolysis.

dence of interaction changed in appearance (Figure 4). No evidence was seen for back-reaction of A with expelled ethene on annealing or on long-wavelength photolysis ($\lambda > 375$ nm).

$WCp_2(C_2H_4)$ was chosen for a UV/vis/near-IR experiment because of the high conversion to A and the weakness of its optical absorptions. UV photolysis revealed the same two product absorptions as observed on photolysis of WCp_2H_2, a structured absorption peaking at 396.6 nm and an unstructured band at 322 nm. The peaks were rendered more conspicuous by subtraction of the spectrum before photolysis (Figure 5). As in the experiment on WCp_2H_2, the 397-nm peak showed fine structure (separations 25–120 cm^{-1}) superimposed on a vibrational progression of mean frequency 320 ± 14 cm^{-1}. When the matrix was annealed, the fine structure sharpened considerably (Figure 1, Table V) and new features could be observed. The fine structure is provisionally assigned to phonon coupling; the zero-phonon (0,0) line may then be the band at 404.8 nm, which appeared on annealing.

WCp_2CO. Exposure of an argon matrix containing WCp_2CO to 1 min of broad-band UV led to a decrease in intensity of starting material bands to 90% of their initial value and the appearance of bands due to A and free carbon monoxide (see Table II). A 2-h photolysis brought about a better than 90% conversion of WCp_2CO into A (see figure of ref 2). In the free-CO stretching region, bands grew at 2137 and 2128 cm^{-1} (Ar matrix) and 2138, 2127, and 2125 cm^{-1} (N_2 matrix). Annealing of the dinitrogen matrix after photolysis caused the bands at 2127 and 2125 cm^{-1} to decrease in intensity with a concomitant increase in the intensity of the band at 2138 cm^{-1}. It was not possible to reverse the photochemical reaction by photolysis with visible light. However, a thermal reaction between A and CO was observed when a xenon matrix was annealed above 50 K (the absorbance of the C–O stretching band of WCp_2CO increased from 0.30 to 0.38 on annealing to 65 K and recooling; free CO at 2133 and 2122 cm^{-1} decreased from 0.09 to 0.04). The structure in the spectrum of the expelled CO and the discrepancy between the observed frequencies and those of monomeric CO (2138.6 cm^{-1} in Ar, 2133.2 cm^{-1} in Xe)[20] can be attributed to perturbation by A.

One experiment was tried using a pure carbon monoxide matrix in an attempt to make the known compound $WCp(\eta^3\text{-}C_5H_5)(CO)_2$.[7,21] Photolysis with $\lambda > 375$ nm gave 50% conversion to product A after 1 h. There was no evidence for the formation of any other carbonyl species under these conditions nor under the other photolysis conditions (254 and 314 nm).

$W(\eta\text{-}C_5D_5)_2H_2$. On 2 h of broad-band UV photolysis of $W(\eta\text{-}C_5D_5)_2H_2$ in Ar, a new set of bands grew at the expense of the starting material (see Table II). These can be assigned to a deuterated version of A: A^d. As a result of the low intensity of the absorptions of A^d only five of its IR-active vibrations were definitely observed.

$W(\eta\text{-}C_5D_5)_2D_2$. Prolonged broad-band UV photolysis of $W(\eta\text{-}C_5D_5)_2D_2$ in Ar was relatively ineffective at bringing about a photoreaction. The only feature of the photoproduct detected was the absorption of A^d at 3225 cm^{-1}.

The results reported above are summarized in Chart II. The bands of A in Ar matrices from the four sources other than $WCp_2(C_2H_4)$ did not differ by more than 2 cm^{-1}, except for one shift of 4 cm^{-1} recorded for the 3240-cm^{-1} band. The reaction products observed in individual experiments and the production of A by several independent routes leaves no doubt that A is WCp_2, tungstenocene. This conclusion receives strong support from the appearance of the IR absorption spectra of A and A^d. The product observed in UV experiments must also be assigned to A for three reasons: (a) only one organometallic product is observed in both UV and IR experiments, (b) the same UV absorptions are observed when WCp_2H_2 and $WCp_2(C_2H_4)$ precursors are used, (c) only a

Chart II

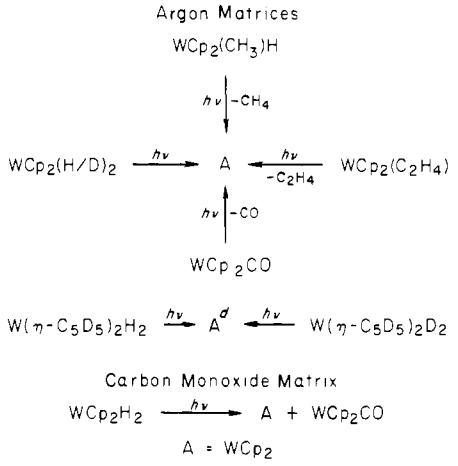

(20) Dubost, H. *Chem. Phys.* **1976**, *12*, 139.
(21) Huttner, G.; Brintzinger, H. H.; Bell, L. G.; Friedrich, P.; Bejenke, V.; Neugebauer, D. *J. Organomet. Chem.* **1978**, *145*, 329.

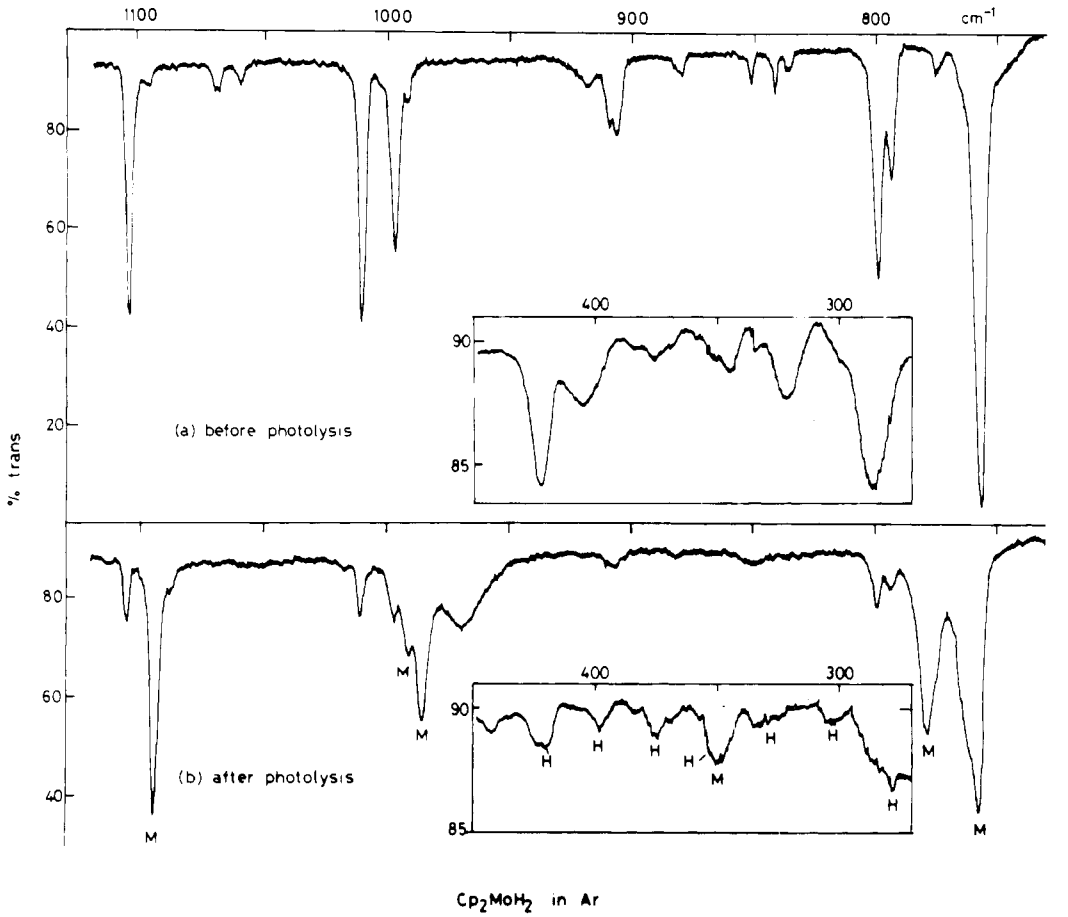

Figure 6. IR spectra recorded (a) following codeposition of $MoCp_2H_2$ and Ar at 20 K and (b) following a subsequent 30-min Hg arc photolysis. Note ×5 ordinate expansion below 450 cm^{-1}; M = $MoCp_2$, and H = residual atmospheric water vapor in spectrometer. Other bands are due to $MoCp_2H_2$.

high-symmetry molecule such as a metallocene would give the observed well-resolved UV spectrum (see Discussion).

$MoCp_2H_2$. A 30-min broad-band UV photolysis of argon matrices containing $MoCp_2H_2$ led to an 80% loss of starting material and the growth of new bands (see Table VII[14] and Figure 6). These bands maintained a constant intensity ratio in different experiments. Taken with other observations described below, this indicates that they should be assigned to a single product M. Under much more dilute conditions, 30 min of photolysis yielded M in better than 90% yield.

When the experiment was repeated using simultaneous spray-on and photolysis, some subtle differences were detected (see Table VII). The main photoproduct was still M, but a number of weak bands were detected, which were assigned to product(s) N. Apparently in the more fluid conditions that exist in the matrix during deposition, a small amount of the photoproduct M reacts with incoming MCp_2H_2 (this is consistent with the known solution photochemistry of $MoCp_2H_2$).[3]

An experiment using UV/vis/near-IR detection to examine the photolysis of $MoCp_2H_2$ in Ar showed decreasing absorption of the starting material on photolysis (Table III) and increasing absorption by the product M (301-nm intense unstructured band, 396-nm intense structured band; Figure 5, Table IV). The position and intensity of the 301-nm band are of limited accuracy because of overlap with the starting material absorption. The band at 396 nm showed a vibrational progression of mean frequency 317 cm^{-1}. Although these figures are almost identical with those of A, the onset of the band was 16 nm to longer wavelength, it reached a maximum in the fifth vibrational conponent rather than the second, and the individual components were much broader. Fine structure on the vibrational components was just discernible but is not tabulated. The extinction coefficients of the product bands are estimated (Table IV) by using the same methods as for the tungsten compounds. No bands were detected between 2600 and 430 nm.

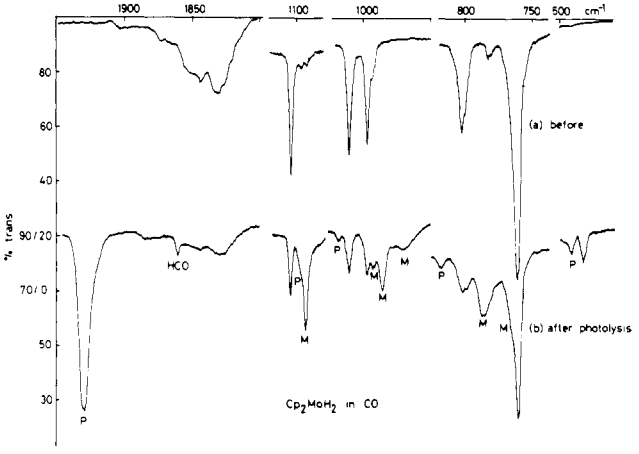

Figure 7. IR spectra recorded (a) following codeposition of $MoCp_2H_2$ and CO at 20 K and (b) after a subsequent 30-min Hg arc photolysis; M = $MoCp_2$, and P = $MoCp_2CO$. Unmarked bands are due to $MoCp_2H_2$.

In CO matrices the main photoproduct of $MoCp_2H_2$ was M, but nine IR bands of $MoCp_2CO$ were also detected (see Tables VI and VII and Figure 7) and a very weak band at 1860 cm^{-1}, assigned to HCO.[15] Spray-on with photolysis in CO gave similar results, but a number of other weak bands appeared that may be assigned to N (see Table VII). On photolysis with $\lambda > 375$ nm for 2.5 h, the bands assigned to

Table VIII. IR Wavenumbers of Metallocenes in Ar Matrices (cm^{-1})[a]

VCp_2	$CrCp_2$	$MoCp_2$	WCp_2	$Mo(\eta\text{-}C_5D_5)_2$	$W(\eta\text{-}C_5D_5)_2$
			3236 vs, br		3225 vs, br
3107 w	3110 w, br	3110 w	3100 w	2343 w	
	3092 vw, br	3092 w	3090 w		
1430 w	1412 vw, br				
1112 m	1099 s, br	1094 s	1086 s	1051 m	1035 m
1110 sh				1038 s	1032 s
	1052 w, br				
1012 sh	994 sh	991 m	981 s	763 s	760 s
1010 s	986 s, br	985 s	971 s		
		970 m, br			
786 sh	785 s, br	778 s	778 s	609 m, br	660 w, br
783 vs					
779 sh					
	756 s, br	761 s		578 s	599 w, br
	716 w			568 s	
429 w	438 m	350 w	324 m	343 w	312 w
385 w			264 m		

[a] Abbreviations: w, weak; m, medium; s, strong; sh, shoulder; br, broad; v, very.

$MoCp_2CO$ decreased in intensity by 50%, those assigned to M increased by about 10%, and those assigned to N remained unchanged in intensity. Photolysis with a 312-nm filter increased the amount of $MoCp_2CO$ at the expense of M, indicating that M is also photosensitive.

$MoCp_2D_2$. Broad-band UV photolysis of an argon matrix containing $MoCp_2D_2$ (80% D in hydridic position) led to a decrease in intensity of bands assigned to starting material and the appearance of bands assigned to M (see Table VII).

$MoCp_2CO$. On 3 min of UV photolysis of $MoCp_2CO$ in argon, IR bands due to starting material decreased to about 30% of their initial value while bands due to M grew along with two bands at 2137 and 2130 cm^{-1} (assigned to free and interacting CO). UV/vis/near-IR spectra measured before and after photolysis of $MoCp_2CO$ in argon revealed the bands of M in almost the same positions as when obtained from $MoCp_2H_2$ (Table IV). The extinction coefficients are estimated in the usual way. The intensity of the 302-nm band relative to that of the 396-nm band appeared greater in the spectra when $MoCp_2CO$ was photolyzed than when $MoCp_2H_2$ was photolyzed. This anomaly is associated with the stronger absorption of $MoCp_2H_2$ at 300 nm; the true relative intensities should be closer to those obtained in the synthesis of M from $MoCp_2CO$.

Photolysis of $MoCp_2CO$ in a xenon matrix followed by annealing was used to test for recombination of M with CO. When the matrix was annealed to 60–65 K and recooled, only marginal evidence was obtained for an increase in absorbance of $MoCp_2CO$. However, when the experiment was repeated using xenon doped with 1% excess CO, a substantial increase was observed in $MoCp_2CO$ absorbance at 1911 cm^{-1} (0.61 before, 0.98 after) and a decrease in CO absorbance at 2136 cm^{-1} (0.75 before, 0.59 after). Thus excess CO allows M to react with CO at 60 K to reform $MoCp_2CO$.

$Mo(\eta\text{-}C_5D_5)_2H_2$ and $Mo(\eta\text{-}C_5D_5)_2D_2$. A 45-min photolysis of $Mo(\eta\text{-}C_5D_5)_2H_2$ in argon matrices led to a decrease of 95% in intensity of starting material bands and the growth of bands assigned to deuterated M; M^d (see Table VII and Figure 8). M^d was also observed on photolysis of $Mo(\eta\text{-}C_5D_5)_2D_2$.

The results reported above are summarized in Chart III. The fact that a common photoproduct was observed from a number of different starting materials, that free carbon monoxide was observed on photolysis of $MoCp_2CO$, and that the spectrum of M was influenced only by deuterating the protons on the cyclopentadienyl rings, indicates that M is molybdenocene, $MoCp_2$. This receives very strong support from the very similar appearance of the IR spectra of M and chromocene (see below). The product observed in the UV experiments must also be assigned to M by using reasoning

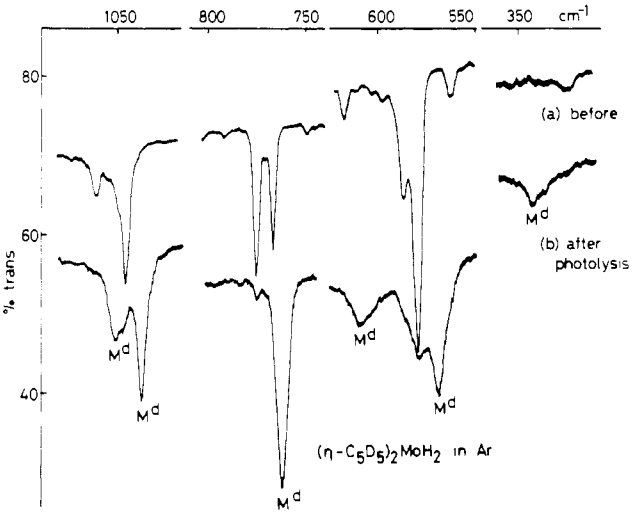

Figure 8. IR spectra recorded (a) following codeposition of $(\eta\text{-}C_5D_5)_2MoH_2$ and Ar at 20 K and (b) after a subsequent 45-min Hg arc photolysis; $M^d = (\eta\text{-}C_5D_5)_2Mo$. Unmarked bands are due to $(\eta\text{-}C_5D_5)_2MoH_2$. Spectrum b is displaced relative to (a) by 20%.

similiar to that given for the assignment of A.

$CrCp_2$. The experiments described above showed that the metallocenes $MoCp_2$ and WCp_2 reacted under photochemical stimulation with carbon monoxide matrices to give the known carbonyl adducts. The corresponding adduct of chromocene has been reported in the literature as a labile species (stable in solution below 0 °C) formed by direct addition of carbon monoxide to a solution of chromocene.[7] It was characterized by ^1H NMR and by the observation of an intense IR band at 1900 cm^{-1}. We attempted to reproduce this result under matrix conditions and to examine the spectra of $CrCp_2$ in matrices.

The IR spectrum of $CrCp_2$ both in Ar and in CO matrices (Table VIII, Figure 9a) shows several features that distinguish it from the spectra of metallocenes with orbitally nondegenerate ground states. All the bands are considerably broader than those observed for other first-row metallocenes under similar deposition conditions (e.g., fwhm of 1100-cm^{-1} band: $CrCp_2$, 6.5 cm^{-1}; VCp_2, 2.5 cm^{-1}). There are two intense bands in the 750–850-cm^{-1} region rather than one as usually observed, and there is only one low-frequency skeletal mode at 438 cm^{-1} instead of the usual pair of bands. UV/vis spectra of $CrCp_2$ in Ar (Figure 5) show features very similar to those observed in solution with no significant sharpening of bands. After 1 h of broad-band UV photolysis of $CrCp_2$ in CO, the

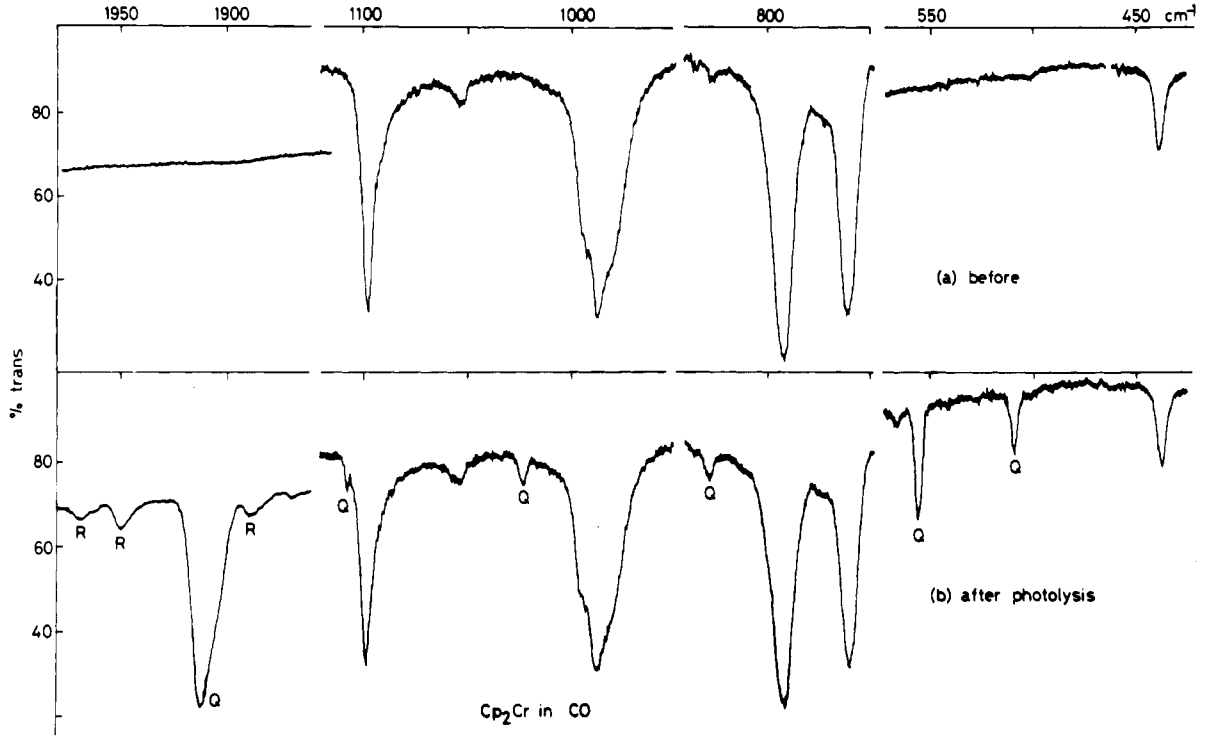

Figure 9. IR spectra recorded (a) following codeposition of $CrCp_2$ and CO at 20 K and (b) after a subsequent 60-min photolysis; Q = $CrCp_2CO$, and R = unidentified polycarbonyl products. Other bands are due to $CrCp_2$.

Chart III

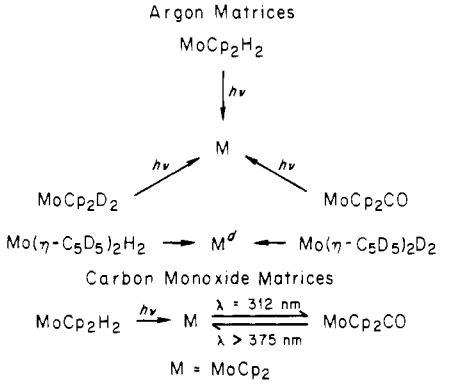

intensities of the starting material bands had decreased by about 10% and several product bands were observed (1970, 1950, 1912, 1889, 1107, 1023, 893, 828, 602, 566, 556, and 510 cm^{-1}; Figure 9b). Most of the product bands may be assigned to $CrCp_2CO$ by analogy with the IR spectra of $MoCp_2CO$ and WCp_2CO (Table VI). Weak features at 1970, 1950, and 1889 cm^{-1} may be accounted for by the formation of a very small amount of some polycarbonyl species, which in turn implies that some decoordination of a cyclopentadienyl ligand had occurred.

VCp_2 and VCp_2CO. The experiments described above in which metallocene–metallocene carbonyl equilibria were studied suffered from the disadvantage that, in two of the cases, the metallocenes could only be generated in situ, while in the third case, the carbonyl could only be generated in situ. The VCp_2/VCp_2CO equilibrium offered a system in which both species were well characterized and therefore provided a valuable check on the feasibility of the proposed matrix reaction.

Vanadocene, like other orbitally nondegenerate metallocenes, showed a sharp IR spectrum (Table VIII). The two low-frequency modes were of comparable intensity, and one intense and one weak feature were observed between 750 and 850 cm^{-1}; the C–H stretching modes were weak and broad. Pyrex-filtered photolysis of vanadocene in a pure CO matrix gave evidence for slight conversion to the carbonyl adduct.

A matrix prepared by cocondensation of VCp_2CO with Ar showed considerable thermal decomposition to VCp_2 and CO (2138 cm^{-1}). On photolysis of the matrix for 7 min with broad-band UV, the absorptions due to the starting material were almost completely eliminated while those due to VCp_2 increased in intensity dramatically (Figure 10). The carbon monoxide stretching region showed the presence of two bands at 2138 and 2134 cm^{-1}, which can be assigned to free CO and "interacting" CO (compare with the tungsten system). Neither annealing the matrix nor photolyzing with visible light reversed the reaction.

Discussion

Organometallic Products. The generation of a common product by UV photolysis of a variety of MCp_2L_n precursors in Ar matrices demonstrates conclusively that the products are WCp_2 (A) and $MoCp_2$ (M). In accordance with this conclusion the spectra of the products are unaffected by ^2H substitution of the hydridic hydrogens but substantially altered by substitution of the ring hydrogens. The lack of thermal back-reactions below 50–60 K and the stability of the products in matrices give a strong hint that there is a change from a bent to a parallel ring structure on expulsion of the ligands, so setting up an appreciable barrier to recombination. Other evidence for a parallel structure comes from analysis of the spectra (see below).

In these experiments the lack of effect of dilution is consistent with monomeric products, but for some of the reactions, notably of WCp_2H_2, the conversion to product is below 50%. Use of simultaneous photolysis and deposition increases the yield up to 100% for WCp_2H_2 without the introduction of any other products. However, the use of this technique on $MoCp_2H_2$ introduces a new species, N, which is tentatively identified as a $[MoC_{10}H_{10}]_2$ dimer.[3]

Carbon monoxide is the only matrix that has so far proved reactive toward the metallocenes. Photolysis of WCp_2H_2 in CO gives a low yield of WCp_2CO in addition to WCp_2. The

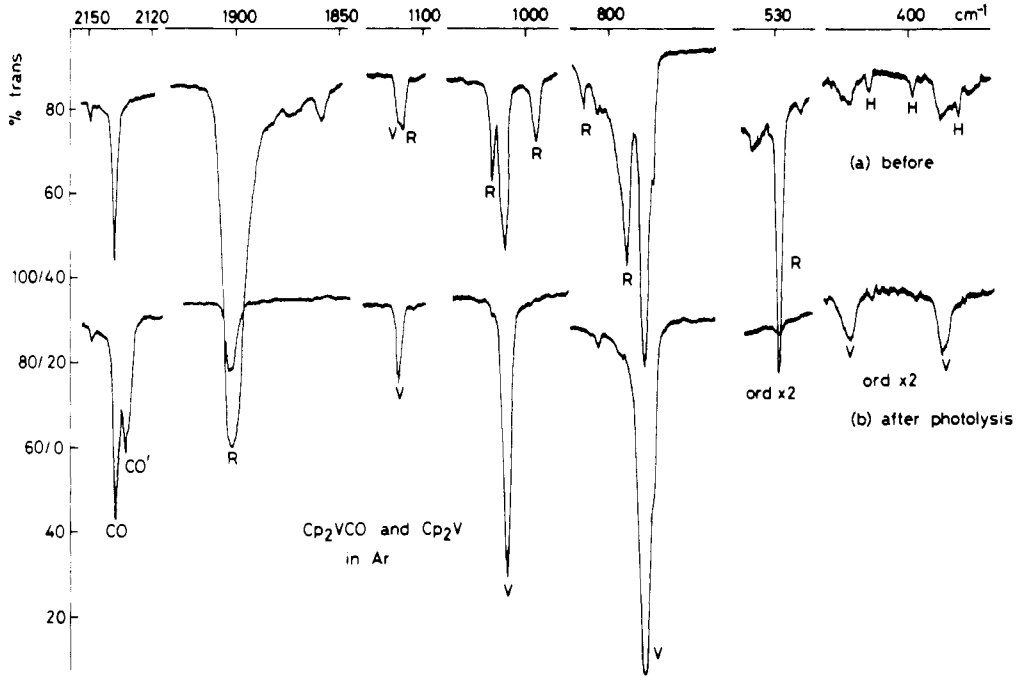

Figure 10. IR spectra recorded (a) following deposition of a sample of VCp_2CO and Ar (note substantial thermal decomposition to VCp_2 and CO has occurred during deposition) and (b) after a subsequent 7-min Hg arc photolysis. Note ×2 ordinate expansion below 600 cm^{-1}. CO′ = perturbed CO, R = VCp_2CO, V = VCp_2, and H = residual atmospheric water vapor.

carbonyl adduct is identified by the coincidence of the CO stretching mode with that of an authentic sample in a CO matrix. Photolysis of $MoCp_2H_2$ in CO gives rather higher yields of $MoCp_2CO$ identified by the presence of nine IR bands within 5 cm^{-1} of those of a sample of $MoCp_2CO$ in Ar. Pyrex-filtered photolysis of vanadocene gives a low yield of a carbonyl, probably VCp_2CO, absorbing at 1892 cm^{-1} (compare VCp_2CO in Ar: 1903 cm^{-1}). UV photolysis of chromocene gave appreciable conversion to a product with a CO stretching mode at 1912 cm^{-1} and eight further IR bands that may readily be assigned to $CrCp_2CO$ by comparison with the spectra of MCp_2CO (M = V, Mo, W). The lack of product bands between 975 and 1000 cm^{-1}, and between 750 and 800 cm^{-1}, where other MCp_2CO species absorb, is readily explained by the strong absorptions of chromocene in these regions.

Expelled Ligands. The identification of the expelled ligands CO, CH_4, and C_2H_4 from known matrix spectra is straightforward. The absence of CH_3 absorptions suggests concerted expulsion of methane from $WCp_2(CH_3)H$. Since neither H_2 nor H may be observed directly by IR detection, we used the well-established reaction of hydrogen atoms with CO to form HCO as a test for the presence of hydrogen atoms.[22] Photolysis of WCp_2H_2 in a CO matrix yielded no evidence for HCO absorption at 1860 cm^{-1}, while a similar experiment with $MoCp_2H_2$ yielded a weak absorption due to HCO. In this experiment, the HCO absorbance was 20% that of $MoCp_2$ at 1093 cm^{-1}. Since the matrices used for these experiments were more concentrated than most, it is uncertain whether HCO was produced in the primary reaction of $MoCp_2H_2$ or by secondary photolysis of N. In comparable experiments with $ReCp_2H$ in CO, substantially higher yields of HCO were obtained both in absolute terms and relative to the $ReCp_2$ product.[23] We conclude that ejection of H_2 from WCp_2H_2 is essentially concerted, while matrix photolysis of $MoCp_2H_2$ yields mostly H_2 with a possibility of a minor proportion of hydrogen atoms (cf. solution results).[8]

Matrix isolation has been used frequently to investigate the mutual vibrational interaction of cage pairs. In some photochemical experiments the products are observed as a cage pair, for instance $CO\cdots Fe(CO)_4$,[24] $CO\cdots Cr(CO)_5$,[25] and $CF_4\cdots SF_2$.[26] In our experiments the CO expelled from MCp_2CO (M = V, Mo, W) (Figure 10, Tables II and VII) appeared as doublets. In each case the high-frequency component was close to the 2138.6-cm^{-1} band of monomeric CO, while the other component was 4–11 cm^{-1} to lower wavenumbers. In xenon the components were unresolved but the band was exceptionally broad. The high-wavenumber component must be assigned to "free" CO, which has escaped the cage, while the low-frequency component is assigned to a $CO\cdots MCp_2$ cage pair. The behavior observed on annealing N_2 matrices is consistent with this assignment. It is unusual for the CO frequency to be shifted to low wavenumber by such interactions; interactions with H_2O, CO_2, CO,[20] and $Fe(CO)_4$ all shift it to high wavenumbers. There are no corresponding bands of the metallocenes which appear as doublets, but there is a 4-cm^{-1} shift in the band of WCp_2 at 3240 cm^{-1} when generated from WCp_2CO rather than WCp_2H_2.

The spectrum of expelled ethene and tungstenocene generated from $WCp_2(C_2H_4)$ reveals a more extensive perturbation pattern which changes appreciably on annealing (Figure 4, Table II). While ν_7 of ethene shows a 10-cm^{-1} shift to high wavenumber, ν_{12} is shifted 5 cm^{-1} down in the cage complex. The shift of 32 cm^{-1} to high wavenumbers of the 3240-cm^{-1} band of WCp_2 is exceptionally large. Fredin and Nelander, who examined the $C_2H_4\cdot Cl_2$ complex,[27a] also found ν_7 to be the most sensitive ethene mode. The observation of these cage pairs between MCp_2 and expelled CO or C_2H_4 reinforces the arguments for a parallel ring structure for the metallocenes. With such a structure the stability of the cage pairs toward recombination can be understood readily. This situation contrasts with that found for $MCp_2(H)(CO)$ (M = Nb, Ta)

(22) See, e.g.: Guillory, W. A.; Andrews, G. H. *J. Chem. Phys.* **1975**, *62*, 3208.
(23) Chetwynd-Talbot, J.; Grebenik, P.; Perutz, R. N. *J. Chem. Soc., Chem. Commun.* **1981**, 452.
(24) Poliakoff, M.; Turner, J. J. *J. Chem. Soc., Dalton Trans.* **1973**, 1351.
(25) Perutz, R. N.; Turner, J. J. *J. Am. Chem. Soc.* **1975**, *97*, 4791.
(26) Willner, H. *Z. Anorg. Allg. Chem.* **1981**, *481*, 117.
(27) (a) Fredin, L.; Nelander, B. *J. Mol. Struct.* **1973**, *16*, 205. (b) Chetwynd-Talbot, J.; Grebenik, P.; Perutz, R. N., unpublished observations.

when no evidence is found for interaction between the photoproduct $MCp_2(H)$ and the expelled CO.[27b] Here we conclude that the product has nonparallel rings and is unstable toward recombination unless the CO has diffused out of the cage.

IR Spectra of MCp_2 (M = Cr, Mo, W). The matrix IR spectra of chromocene and molybdenocene are remarkably similar but different from those of tungstenocene or other metallocenes (Figures 6 and 9a, Table VIII). Both show two intense broad bands between 750 and 800 cm^{-1} and only one low-frequency skeletal mode. These spectra are drastically simpler than those of MCp_2CO in the crucial 700–1200-cm^{-1} region, which involves only vibrations of the hydrocarbon ligands, strong confirmatory evidence for the parallel ring structure for molybdenocene predicted by Brintzinger et al.[6] Further support comes from the magnitudes of the shifts observed on deuteration, which agree closely with those of ferrocene.[28]

The most intense band in the IR spectrum of tungstenocene is the broad feature at 3240 cm^{-1}, which is shifted only 15 cm^{-1} on ^2H substitution of the ring hydrogens. Since this is inconsistent with any vibrational transition, we assign it to an electronic transition, the nature of which is discussed in the next section. The remaining features in the IR spectrum closely resemble those of the orbitally nondegenerate metallocenes (compare VCp_2, Figure 10, and WCp_2, Figure 2), and the shifts observed on deuteration are in line with those of ferrocene[28] (Table VIII). The main differences are that ν_{18} is a doublet in all matrices used (Ar, Xe, N_2, CO, CH_4) and that the two skeletal modes appear at low frequency relative to those of osmocene.[29] The similarities in number, frequencies, and intensities of the bands of WCp_2 and $W(\eta\text{-}C_5D_5)_2$ to those of the other metallocenes provide strong circumstantial evidence for a parallel sandwich formulation for this molecule. However, the differences between the spectra of WCp_2 and its congeners in group 6 point to a significant change in electronic state.

Electronic Spectra and Ground State of MCp_2 (M = Cr, Mo, W). Brintzinger et al.[6] and Warren[30] have analyzed the possible ground states of the d^4 metallocenes. Of the three possibilities $^1A_{1g}$ (e_{2g}^4), $^3A_{2g}$ $(a_{1g}^2e_{2g}^2)$, and $^3E_{2g}$ $(a_{1g}^1e_{2g}^3)$, chromocene adopts the $^3E_{2g}$ ground state.[30] The $^1A_{1g}$ state may be excluded for the other d^4 metallocenes on electron repulsion grounds, but both $^3A_{2g}$ and $^3E_{2g}$ states are energetically feasible ground states. The most likely state, $^3E_{2g}$, is additionally subject to Jahn–Teller and spin–orbit splitting. The effect of spin–orbit coupling on the ^3E state and the associated ^1E state is considered first. Evaluation of the secular determinant containing the matrix elements given by Warren[30] yields the four solutions shown in Figure 11. The Jahn–Teller distortion modes of an E_2 state should belong to the e_1 representation. Spin-orthogonality arguments show that the diagonal Jahn–Teller effect operates only on two of the four spin–orbit eigenstates, F_2 and F_4.

The ground state of WCp_2 may be deduced from the presence of the 3240-cm^{-1} electronic transition. This band is broad by vibrational standards but not for an electronic transition (fwhm = 29 cm^{-1} in Ar, 26 cm^{-1} in CO) and shows no vibrational progression. An order of magnitude estimate of the oscillator strength was made by isolating the WCp_2CO in a mixed Ar/CO (1200:1) matrix and using the CO as an internal calibrant. This method gave an extinction coefficient of 500 dm^3 mol^{-1} cm^{-1}, an oscillator strength of 5×10^{-5}, and a matrix ratio of WCp_2CO/Ar of 1:800. These figures are

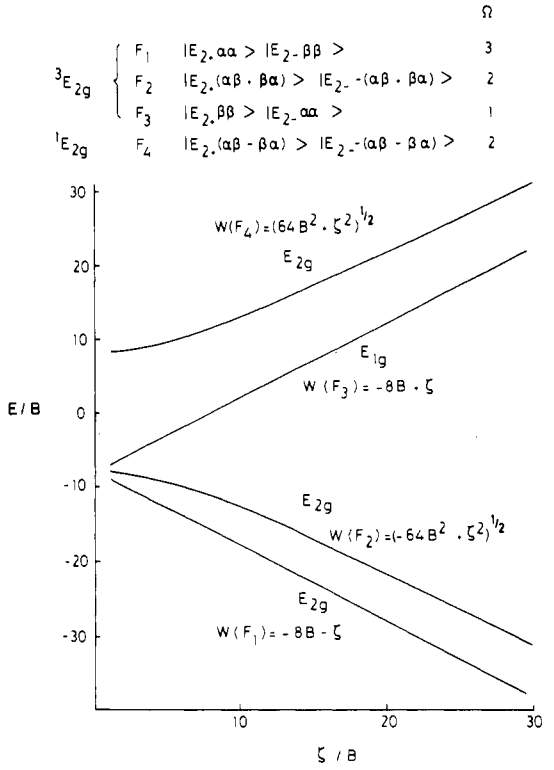

Figure 11. Calculated effect of spin–orbit coupling on $^3E_{2g}$ and $^1E_{2g}$ energy levels of WCp_2. The four spin–orbit functions are labeled F_1–F_4 and their energies $W(F_1)$–$W(F_4)$; B = Racah electron repulsion parameter, ζ = spin–orbit coupling constant, and Ω = orbital angular momentum quantum number.

consistent with a d–d electric dipole transition.[31] There are two types of low-energy electronic transitions possible, inter- and intraconfigurational transitions. The only spin-allowed interconfigurational transition (^3A–^3E) should have energy $\Delta_2 - 8B$, probably slightly higher than that observed. However, the absence of a vibrational progression is inconsistent with the expected change in geometry for this transition. Intraconfigurational transitions become possible from a $^3E_{2g}$ ground state when the spin–orbit interaction is considered (see Figure 11). Transitions from F_1 to F_2 and F_4 are spin forbidden and would occur only via a magnetic dipole mechanism, such that the lower frequency band (~500 cm^{-1}) should have the greater intensity. Calculations using eq 11.4 from ref 32 show that the oscillator strength should be $\sim 10^{-7}$ rather than $\sim 10^{-5}$ as observed. The only spin-allowed electric dipole transition is F_3–F_1 (energy 2ζ). With estimation of B as ~200 cm^{-1} (cf. $RuCp_2$, B = 260 cm^{-1})[33] and ζ as 1500 cm^{-1} (cf. $W(\eta\text{-}C_6H_6)_2^+$, ζ = 1730 cm^{-1}),[34] the transition F_3–F_1 has an energy of appropriate magnitude. The transition F_2–F_1 cannot lie at 3240 cm^{-1}, while F_4–F_1 would require values of B and ζ of ~80 and ~1200 cm^{-1}, respectively.

The F_3–F_1 transition may be stimulated by a vibronic mechanism with enabling vibrations of symmetry e_{2u}, e_{1u}, a_{1u}, or a_{2u}. If the enabling vibration is one of the skeletal modes ν_{11}, ν_{21}, or ν_{22}, ζ must be in the range $1450 < \zeta < 1570$ cm^{-1}. The effect of deuteration may then represent the difference in frequency of the enabling vibration between WCp_2 and $W(\eta\text{-}C_5D_5)_2$. This type of transition is consistent with the observed transition energy, the estimated oscillator strength,

(28) Lippincott, E. R.; Nelson, R. D. *Spectrochim. Acta* **1958**, *10*, 307.
(29) Lokhsin, B. V.; Aleksanian, V. T.; Rusach, E. B. *J. Organomet. Chem.* **1975**, *86*, 253.
(30) Warren, K. D. *Struct. Bonding (Berlin)* **1976**, *27*, 45.
(31) Lever, A. B. P. "Inorganic Electronic Spectroscopy"; Elsevier: Amsterdam, 1968.
(32) Griffith, J. S. "The Theory of Transition Metal Ions"; Cambridge University Press: Cambridge, England, 1961.
(33) Sohn, Y. S.; Hendrickson, D. N.; Gray, H. B. *J. Am. Chem. Soc.* **1971**, *93*, 3603.
(34) Green, J. C. *Struct. Bonding (Berlin)* **1981**, *43*, 37.

the absence of vibrational progression, and the absence of bands in this region for chromocene and molybdenocene. Transitions in the infrared within the spin–orbit manifold have been observed previously in MF_6 (M = Re, Os, Ir, Pt)[35] and in $[MX_6]^{2-}$ (X = Cl, Br; M = Os, Ir).[36]

The similarity of the IR spectrum of WCp_2 to those of orbitally nondegenerate metallocenes may now be understood since the large spin–orbit coupling will quench the Jahn–Teller effect, which does not operate directly on F_1. The spin–orbit coupling constant of Mo is about 25% of that of W and in chromium is reduced still further.[32] The Jahn–Teller stabilization for $MoCp_2$ and $CrCp_2$ may exceed the spin–orbit stabilization leading to dynamic distortions of the ground state. These considerations may explain the broad bands and unusual intensities of the IR bands of these molecules and the absence of bands corresponding to the 3240-cm^{-1} band of WCp_2. We have considered the possibility that the broad band of $MoCp_2$ at 970 cm^{-1} may be the counterpart of the 3240-cm^{-1} band of WCp_2 (giving $\zeta_{Mo} \approx 0.25\zeta_W$). However there is no sign of a corresponding band in $Mo(\eta\text{-}C_5D_5)_2$.

Both molybdenocene and tungstenocene exhibit two further electronic absorptions in the near-UV with oscillator strengths of $(0.8\text{–}2.5) \times 10^{-2}$, indicating that these are fully allowed charge-transfer bands. No bands are observed in the UV/vis region that can be assigned to d–d transitions. Our spectra of chromocene show slight blue shifts relative to the published solution spectra[37] (cf. the UV/vis spectra of other matrix-isolated metallocenes).[38] The chromocene band at 333 nm has been assigned to a L–M charge-transfer transition on the basis of red shifts on methyl substitution in the rings.[38] The lowest charge-transfer transitions of $MoCp_2$ and WCp_2 occur at wavelengths longer than that of $CrCp_2$ and exhibit considerable fine structure. At this point, we have no strong evidence regarding the direction of charge transfer. The progression frequencies of 320 cm^{-1} for both WCp_2 and $MoCp_2$ must be assigned to a gerade vibrational mode; either a_{1g} (ν_4) or less likely the e_{1g} (ν_{16}) skeletal mode.[39] These excited-state frequencies may be compared to the ground-state a_{2u} and e_{1u} modes measured by IR spectroscopy (W, 325 and 265 cm^{-1}; Mo, 350 cm^{-1}). Such well-resolved fine structure is itself indicative of a high-symmetry structure. Similar fine structure has been observed for ferrocene[38] but not for bent MCp_2L_n systems.

Photochemical Processes. In the synthesis of molybdenocene and tungstenocene we have observed photoelimination of H_2, D_2, CH_4, CO, and C_2H_4. The elimination of H_2 and CH_4 has been shown to predominate over sequential elimination of 2 H or of CH_3 + H, although there is evidence for some hydrogen atom production from $MoCp_2H_2$. Another example of H_2 elimination from metal hydrides in matrices has been recorded recently for $FeH_2(CO)_4$,[40] but elimination of CH_4 from a $H_3C[E]H$ (E = element) is new to matrix isolation. The reverse reaction, oxidative addition of CH_4 to form M-(CH_3)H, has been observed for several transition-metal atoms.[41] Such concerted reactions, common to many polyhydrides, may involve considerable bond making in the transition state. Bond making is also indicated by the ability to generate $MoCp_2$ in solution from $MoCp_2H_2$ at 366 nm in a monophotonic process, a wavelength that may otherwise be too long to cleave both Mo–H bonds. Such a reaction is consistent with population (either directly or by internal conversion) of the $2a_1$ ligand-field orbital (see Scheme 7 of ref 42), which is $[M]H_2$ antibonding and H–H bonding. In keeping with the solution quantum yields, $MoCp_2H_2$ proved more photosensitive than WCp_2H_2. However, $WCp_2(C_2H_4)$ and MCp_2CO (M = Mo, W) were much more photosensitive than either hydride.

In addition to photoelimination reactions we have observed photoaddition of CO to the metallocenes of chromium and molybdenum and probably those of vanadium and tungsten. The addition of CO to $MoCp_2$ has been observed directly, but the addition to WCp_2 has been detected only when combined with loss of H_2 from WCp_2H_2. Simple photochemical addition reactions of the metallocenes have not been reported previously. The reaction may proceed via population of the e_{1g} ligand field orbital, which is stabilized by bending the rings to a nonparallel position.[42]

Thermal Reaction of MCp_2 with CO. The only thermal reaction that we observed in these matrix experiments was the recombination of MCp_2 (M = Mo, W) with CO in Xe matrices following photolysis of MCp_2CO and annealing to 50–65 K. This reaction required excess CO (1%) with molybdenocene but not with tungstenocene. Annealing of more volatile matrices (Ar, N_2, CO, CH_4) had no effect. These observations suggest an appreciable barrier toward ring bending and recombination, with a slightly higher barrier for Mo than for W. Neither thermal nor photochemical reactions have been observed between WCp_2 and N_2 or between WCp_2 and C_2H_4 despite excess reagent in both cases.

Nature of C–H Activation Process. The experiments that we have reported demonstrate that MCp_2 (M = Mo, W) is generated as the primary photoproduct in matrices from a variety of precursors. These metallocenes have been postulated as the crucial "high-energy" reaction intermediates in the C–H activation reactions of precursors such as WCp_2H_2.[2–6] Our experiments provide strong evidence in favor of this pathway, although we have not been able to demonstrate the second stage of the reaction, oxidative addition to the metallocenes. Our experiments do cast some light on the differences in reactivities of molybdenocene and tungstenocene toward C–H insertion. One possible explanation, a higher activation energy of the metallocene toward bending, seems very unlikely since we have observed the thermal reaction of $MoCp_2$ at a temperature as low as 60 K. The change we have observed in the electronic ground state of the metallocenes $MoCp_2$ and WCp_2 offers a second possible explanation. However, we consider this change to be too slight to tip the balance. The third possibility that the $MoCp_2(R)H$ (R = Ph, alkyl, etc.) compounds are too unstable photochemically and/or thermally to be detected in room-temperature experiments is not susceptible to direct test by our matrix experiments. This explanation appears to be the most plausible.

Conclusions

We have shown that monomeric MCp_2 (M = Mo, W) may be generated by photochemical dissociative reactions in low-temperature matrices. The photochemical reactions proceed by concerted reductive elimination (H_2, CH_4) or ligand photodissociation (CO, C_2H_4). The metallocenes are shown to have parallel structures on the basis of their reactivity toward recombination with expelled ligands and the characteristics of their IR and UV/vis spectra. While molybdenocene most closely resembles chromocene in its IR spectrum and may show

(35) Moffitt, W.; Goodman, G. L.; Fred, M.; Weinstock, B. *Mol. Phys.* **1959**, *2*, 109.
(36) Allen, G. C.; Al-Mobarak, R.; El-Sharkawy, G. A. M.; Warren, K. D. *Inorg. Chem.* **1972**, *11*, 787. Flint, C. D.; Paulusz, A. G. *Ibid.* **1981**, *20*, 1768.
(37) Gordon, K. R.; Warren, K. D. *Inorg. Chem.* **1978**, *17*, 987.
(38) Smith, J. J.; Meyer, B. *J. Chem. Phys.* **1968**, *48*, 5436. Barton, T. J.; Douglas, I. N.; Grinter, R.; Thomson, A. J. *J. Chem. Soc., Dalton Trans.* **1976**, 1948. Barton, T. J.; Grinter, R.; Thomson, A. J. *Ibid.* **1979**, 1912.
(39) Fritz, H. P. *Adv. Organomet. Chem.* **1964**, *1*, 239.
(40) Sweany, R. L. *J. Am. Chem. Soc.* **1981**, *103*, 2410.
(41) Billups, W. E.; Konarski, M. M.; Hauge, R. H.; Margrave, J. L. *J. Am. Chem. Soc.* **1980**, *102*, 7393. Ozin, G. A.; McIntosh, D. F.; Mitchell, S. A. *Ibid.* **1981**, *103*, 1574.
(42) Lauher, J. W.; Hoffmann, R. *J. Am. Chem. Soc.* **1976**, *98*, 1729.

dynamic Jahn-Teller distortions of a ^3E ground state, tungstenocene bears a closer resemblance to the orbitally nondegenerate metallocenes. Both metallocenes exhibit intense charge-transfer bands in the near-UV, but tungstenocene shows an additional sharp electronic transition at $\sim$3240 cm^{-1}, which is assigned to a transition between two spin-orbit substates. We conclude that Jahn-Teller activity of tungstenocene is quenched by spin-orbit coupling.

A substantial fraction of the expelled ligands CO and C_2H_4 stays within the same matrix cage as the metallocene, resulting in mutual perturbation of IR and UV spectra. On annealing these expelled ligands diffuse away without recombining. However, both heavy metallocenes (M = Mo, W) react thermally with CO in the 50–65 K region in a Xe matrix. All the group 6 metallocenes react photochemically with CO to give the carbonyls MCp_2CO.

Acknowledgment. We are grateful to Drs. P. A. Cox, A. J. Downs, and M. L. H. Green for many discussions and for use of their apparatus. We thank SERC for support and for a studentship (P.G.) and Dr. G. P. Gaskill for preliminary studies.

Note Added in Proof. Since submitting this manuscript, we have conducted magnetic circular dichroism experiments on MCp_2 (M = Mo, W) in matrices. The resulting spectra show an intense C term, thus confirming that these metallocenes are paramagnetic. Details will be published elsewhere.

Registry No. WCp_2H_2, 1271-33-6; WCp_2D_2, 11082-26-1; $WCp_2(CH_3)H$, 72415-89-5; $WCp_2(C_2H_4)$, 37343-06-9; WCp_2CO, 39333-44-3; $MoCp_2H_2$, 1291-40-3; $MoCp_2D_2$, 11082-25-0; $MoCp_2CO$, 12701-85-8; $W(\eta\text{-}C_5D_5)_2H_2$, 82482-36-8; $W(\eta\text{-}C_5D_5)_2D_2$, 82482-37-9; $Mo(\eta\text{-}C_5D_5)_2H_2$, 82482-38-0; $Mo(\eta\text{-}C_5D_5)_2D_2$, 82482-39-1; WCp_2, 51481-44-8; $MoCp_2$, 51370-80-0; VCp_2, 1277-47-0; $CrCp_2$, 1271-24-5; CH_4, 74-82-8; CO, 630-08-0; C_2H_4, 74-85-1; Ar, 7440-37-1.

Supplementary Material Available: Sublimation temperatures (Table I) and frequency listings (Tables II–VII) (7 pages). Ordering information is given on any current masthead page.

Contribution from the Richard B. Wetherill Laboratory, Purdue University, West Lafayette, Indiana 47907

Addition Compounds of Alkali Metal Hydrides. 22. Convenient Procedures for the Preparation of Lithium Borohydride from Sodium Borohydride and Borane-Dimethyl Sulfide in Simple Ether Solvents

HERBERT C. BROWN,* YONG MOON CHOI,[1] and S. NARASIMHAN[1]

Received March 25, 1982

The preparation of $LiBH_4$ in various ether solvents from the readily available reagents $NaBH_4$ and lithium halides is described. The reactivity of lithium halides toward the metathesis reaction generally follows the order LiBr > LiI > LiCl. The heterogeneous reactions proceed satisfactorily with vigorous magnetic stirring. However, attempting to increase the scale of the preparations utilizing mechanical stirrers resulted in incomplete reactions and decreased yield. On the other hand, when the heterogeneous mixture was stirred with mechanical stirrers fitted with Teflon paddles and a mass of glass beads, the rate of the reaction increased considerably, producing quantitative yields of $LiBH_4$ in greatly decreased reaction times. The ease of conversion of $NaBH_4$ into $LiBH_4$ in various solvents follows the order isopropylamine > 1,3-dioxolane > monoglyme > tetrahydrofuran $\approx$ ether. The isolation of solvent-free $LiBH_4$ from the various solvates was attempted under different conditions. In most cases, normal distillation at 100 or 150 °C produced a strong 1:1 solvate, $LiBH_4$·solvent. Only in the case of ethyl ether is the solvent of solvation readily removed at 100 °C at atmospheric pressure. In the other cases, both higher temperatures, up to 150 °C, and lower pressures, down to 0.1 mm, are required to produce the unsolvated material. Thus the ease of isolating unsolvated $LiBH_4$ is ethyl ether > IPA > THF > 1,3-D $\approx$ MG. Consequently, ethyl ether is the medium of choice for the preparation of $LiBH_4$ by the metathesis of $NaBH_4$ and LiBr. $LiBH_4$ can also be conveniently prepared by the reaction of LiH with H_3B·SMe_2 in ethyl ether. Dimethyl sulfide is readily removed, along with ethyl ether of solvation, at 100 °C (atmospheric pressure). These procedures make $LiBH_4$ readily available.

Lithium borohydride is a selective and more reactive reducing agent than sodium borohydride, much more soluble in a variety of organic solvents than the sodium salt. It was first made on a small scale by the action of gaseous diborane or aluminum borohydride on ethyllithium in benzene solutions (eq 1 and 2).[2] Alternatively, in the presence of diethyl ether,

$$3LiC_2H_5 + 2B_2H_6 \rightarrow 3LiBH_4 + (C_2H_5)_3B \quad (1)$$

$$3LiC_2H_5 + Al(BH_4)_3 \rightarrow 3LiBH_4 + (C_2H_5)_3Al \quad (2)$$

diborane is quantitatively absorbed by lithium hydride with the formation of the monoetherate of lithium borohydride in a state of high purity[3] (eq 3).

$$2LiH + B_2H_6 + 2(C_2H_5)_2O \xrightarrow{Et_2O} 2LiBH_4\cdot Et_2O \quad (3)$$

Sodium borohydride is currently manufactured on a large scale and is a comparatively economical reagent. On the other hand, the cost of lithium borohydride is prohibitive for normal application in preparative reductions. Hence, it is desirable to have a convenient procedure to convert sodium borohydride into lithium borohydride.

The first synthetic procedure for the preparation of lithium borohydride by metathesis was reported by Schlesinger, Brown, and Hyde.[4] The reaction of sodium borohydride and lithium chloride was carried out in isopropylamine under reflux for 3 h (eq 4). (Both sodium borohydride and lithium chloride

$$NaBH_4 + LiCl \rightarrow LiBH_4 + NaCl \quad (4)$$

are soluble in isopropylamine.) It was difficult to remove

(1) Postdoctoral research associates on Grant ARO-DAAG-29-79-C-0027, supported by the U.S. Army Research Office.
(2) Schlesinger, H. I.; Brown, H. C. *J. Am. Chem. Soc.* **1940**, *62*, 3429.
(3) (a) Elliott, J. R.; Boldebuck, E. M.; Roedel, G. F. *J. Am. Chem. Soc.* **1952**, *74*, 5047. (b) Schlesinger, H. I.; Brown, H. C.; Hoekstra, H. R.; Rapp, L. R. *Ibid.* **1953**, *75*, 199.
(4) Schlesinger, H. I.; Brown, H. C.; Hyde, E. K. *J. Am. Chem. Soc.* **1953**, *75*, 209.

0020-1669/82/1321-3657$01.25/0